



Cite this: *RSC Adv.*, 2023, **13**, 19326

## Photocatalytic degradation of imidacloprid using $\text{Ag}_2\text{O}/\text{CuO}$ composites

Saadia Rashid Tariq,<sup>1</sup> <sup>\*a</sup> Zunaira Niaz,<sup>a</sup> Ghayoor Abbass Chotana,<sup>1</sup> <sup>b</sup> Dildar Ahmad<sup>c</sup> and Nazia Rafique<sup>d</sup>

Imidacloprid is one of the most commonly used neonicotinoid pesticides that has been identified as a neurotoxin for various non-target organisms. It binds to the central nervous system of organisms, causing paralysis and eventually death. Thus, it is imperative to treat water bodies contaminated with imidacloprid using an efficient and cost effective method. The present study presents  $\text{Ag}_2\text{O}/\text{CuO}$  composites as excellent catalysts for the photocatalytic degradation of imidacloprid. The  $\text{Ag}_2\text{O}/\text{CuO}$  composites were prepared in different compositions by adopting the co-precipitation method and used as a catalyst for the degradation of imidacloprid. The degradation process was monitored using UV-vis spectroscopy. The composition, structure, and morphologies of the composites were determined by FT-IR, XRD, TGA, and SEM analyses. The effect of different parameters *i.e.* time, concentration of pesticide, concentration of catalyst, pH, and temperature on the degradation was studied under UV irradiation and dark conditions. The results of the study evidenced the 92.3% degradation of imidacloprid in only 180 minutes, which was 19.25 hours under natural conditions. The degradation followed first-order kinetics, with the half life of the pesticide being 3.7 hours. Thus, the  $\text{Ag}_2\text{O}/\text{CuO}$  composite was an excellent cost-effective catalyst. The non-toxic nature of the material adds further benefits to its use. The stability of the catalyst and its reusability for consecutive cycles make it more cost effective. The use of this material may help to ensure an imidacloprid free environment with minimal use of resources. Moreover, the potential of this material to degrade other environmental pollutants may also be explored.

Received 31st March 2023

Accepted 21st June 2023

DOI: 10.1039/d3ra02109b

[rsc.li/rsc-advances](http://rsc.li/rsc-advances)

## Introduction

The environmental pollution caused by industrial and agricultural waste is continuously affecting the global climate. Pesticides are widely used in the agriculture sector to control pests and crop damaging insects. These pesticides are persistent under normal environmental conditions and thus stay in the environment for a very long time, thereby causing many hazardous effects on human health and the environment. Water pollution caused by the excessive use of pesticides is one of the important issues faced nowadays.<sup>1,2</sup>

One of the commonly used pesticides is imidacloprid that belongs to chloro-nicotinic class of pesticides. It was developed in 1986 and since then it has been registered in 120 countries worldwide. It works on the motor neurons of insects and creates the over stimulation of the nervous system which ultimately

leads to the death of insects.<sup>3,4</sup> Fleas on domestic pests can also be treated by the use of imidacloprid. The water solubility of imidacloprid coupled with its excessive and unwise use leads to its emissions into water bodies thereby adversely affecting the aquatic organisms as well as human health. In humans, it can cause loss of consciousness and severe respiratory failure.<sup>5-7</sup> Therefore, it is imperative to find a cost-effective method for the abatement of hazardous pollutants like imidacloprid from water bodies. A number of methods have been reported to mitigate the imidacloprid and similar pesticides from water bodies including bio-degradation, photolysis, ozonation, electro-fenton oxidation and ultrasound assisted degradation.<sup>5,8-10</sup> Bio degradation is one of the important methods to transform imidacloprid but the efficiency of this method is very low.<sup>5</sup> Similarly, the other methods suffer from certain limitations such as the formation of metabolites or the generation of waste that need further processing. In this regard, photocatalytic degradation has been given due consideration during recent years. This method involves the use of metal/metal oxides as the catalyst to facilitate the degradation of pollutants.<sup>11,12</sup>

Semiconductor metal oxide nanoparticles are considered excellent photocatalysts. The process involved mainly depends on the transfer of electrons from the valence band to the

<sup>a</sup>Department of Chemistry, Lahore College for Women University, Jail Road Lahore, 54000, Pakistan. E-mail: saadiarashid74@gmail.com

<sup>b</sup>Department of Chemistry and Chemical Engineering, Syed Babar Ali School of Science & Engineering (SBASSE), Lahore University of Management Sciences (LUMS), Lahore 54792, Pakistan

<sup>c</sup>Department of Chemistry, Forman Christian College (A Chartered University), Lahore, 54000, Pakistan

<sup>d</sup>Pakistan Agricultural Research Council, Islamabad, Pakistan



conduction band on the surface under illumination by a suitable wavelength of light.<sup>13,14</sup> When the light strikes the surface of the semiconductor, the electrons get excited from the valence band to the conduction band by the absorption of photons and create free electron–hole pair. The rate of production of active charge carrier species is directly related to the efficiency of the catalyst. To achieve the maximum activity, the energy of the photon should be higher or equal to the bandgap of the catalyst material.<sup>15,16</sup>

Metal/metal oxide-based nanoparticles show better catalytic activity than bulk materials because they have a high surface-to-volume ratio as compared to their respective molecular or atomic scale materials.<sup>17</sup> Copper oxide (CuO), a p-type semiconductor has gained paramount importance as a photocatalyst due to its high stability, excellent optical and electrical properties as well as low cost of formation.<sup>13,18</sup>

To enhance the photocatalytic properties of metal oxide semiconductors, they are doped with other metal ions exhibiting different bandgap values that create an interface between them and efficiently reduce the recombination rate of photo-generated electron–hole pairs. This method enhances the utility and efficiency of the catalyst to a noticeable extent.<sup>15,19</sup> The incorporation of noble metals has drawn the attention of many scientists due to their fascinating catalytic properties. Doping of silver on CuO can enhance the reactivity and selectivity and produce an excellent photo-catalyst.<sup>20</sup> Thus, present study focused on designing an efficient catalyst *i.e.*, silver oxide (Ag<sub>2</sub>O) doped copper oxide composites for the degradation of widely used pesticide imidacloprid under UV irradiations. The material exhibited low leachability and high stability under aqueous conditions.

## Experimental methodology

The Ag<sub>2</sub>O/CuO composites were prepared with different compositions and used for the degradation of imidacloprid. The kinetics of photocatalytic degradation was determined by Langmuir Hinshelwood kinetic model.

### Quality control and quality assurance

All the chemicals used in the present study were of analytical grade with a purity of 99.9%. The glassware used was properly washed and rinsed with distilled water to remove any impurity adhered to it. Afterward, it was dried for 30 minutes in an electric oven set at 100 °C. A doubly distilled water prepared by (Milli Q) was used throughout the study. The technical grade imidacloprid was provided by Ali Akbar group of industries.

### Preparation of Ag<sub>2</sub>O/CuO composites

The co-precipitation method was adopted to prepare the composites where the weight% of Ag<sub>2</sub>O in Ag<sub>2</sub>O/CuO composites was kept at 1.5, 3.0, and 5.0. For this purpose, different amounts of silver nitrate (0.0038, 0.0076, and 0.0127 g) were added to copper nitrate solutions separately and dissolved completely. Afterward 0.1 M ammonium bicarbonate was added dropwise until no more precipitation occurred. The precipitates

were collected and dried at 80 °C in an electric oven for 30 minutes. Finally, the calcination of dried precipitates was carried out in a furnace at 400 °C for 2 hours.<sup>21</sup> The prepared Ag<sub>2</sub>O/CuO composites were characterized by XRD, FTIR, SEM and TG analyses, and employed as catalyst for the photocatalytic degradation of imidacloprid.

### Photocatalytic degradation of imidacloprid

The solutions of different concentrations of imidacloprid (10, 20, 30, 40, and 50 mg L<sup>-1</sup>) were prepared to study the photocatalytic degradation of imidacloprid. These solutions were stirred under UV light in the presence of Ag<sub>2</sub>O/CuO composite for specific time intervals and then analyzed by a UV-visible spectrophotometer (LABOMED, INC, model no: "UVD-3200") at 268 nm for determining the left over concentration of pesticide after degradation. The same process was also performed under dark. The blank experiments were carried out in the absence of Ag<sub>2</sub>O/CuO composite. The effect of various parameters was also studied on the degradation of the aqueous solution of imidacloprid. These included: irradiation time, pesticide concentration, dose of catalyst, pH, and temperature.

The effect of UV irradiation time on the photocatalytic degradation was studied by stirring the imidacloprid solution for different time intervals *i.e.*, 60, 120, 180, 240, and 300 minutes in the presence catalyst under UV light. The effect of the initial concentration of pesticide was studied by preparing different concentrations *i.e.*, 10 mg L<sup>-1</sup>, 20 mg L<sup>-1</sup>, 30 mg L<sup>-1</sup>, 40 mg L<sup>-1</sup> and, 50 mg L<sup>-1</sup> of imidacloprid solution. A 0.01 g portion of Ag<sub>2</sub>O/CuO catalyst was added to a 50 mL volume of each of these solutions. The samples were stirred for a specific time interval in the presence of UV light and analyzed for imidacloprid concentration. The similar control experiments were performed in the dark. Various amounts of Ag<sub>2</sub>O/CuO composite *i.e.*, 0.01 g, 0.02 g, 0.03 g, 0.04 g and, 0.05 g were added to 50 mL volumes of imidacloprid solutions to study the effect of catalyst dose on degradation under UV light for a specific time interval.

The effect of pH was studied by maintaining the pH of imidacloprid solution at 3, 5, 7, 9, and 11 by adding HCl or NaOH solutions, in the presence of 0.01 g of catalyst. The stirring of the prepared solution was continued for an optimum time in the presence of UV light as well as dark. The effect of temperature on photocatalytic degradation of imidacloprid solution was studied by varying temperature of pesticide solution from 20 °C–40 °C in the presence of 0.01 g catalyst. The reusability of the catalyst was studied for three consecutive cycles by regenerating the catalyst. The stability of the catalyst was also studied by carrying out the leaching experiments.

## Results and discussion

The study focused on the degradation of imidacloprid in the presence of Ag<sub>2</sub>O/CuO composite. The UV-visible spectra of imidacloprid (Fig. 1) depicted its  $\lambda_{\text{max}}$  to be 268 nm which is consistent with literature value.<sup>22</sup> This  $\lambda_{\text{max}}$  of 268 nm was used throughout the study for the determination of pesticide concentration during different sets of experiments.



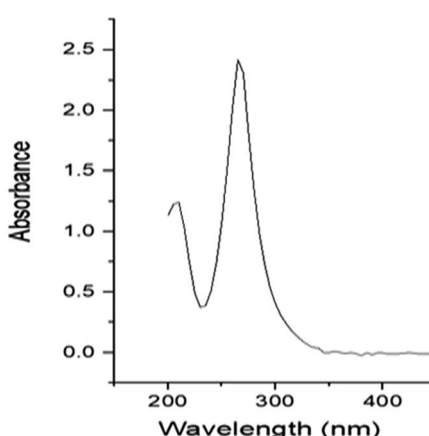


Fig. 1 UV-vis absorption spectra of imidacloprid.

### Characterization of $\text{Ag}_2\text{O}/\text{CuO}$ composites

All the three  $\text{Ag}_2\text{O}/\text{CuO}$  composites were characterized by XRD, FTIR, TG, and SEM analysis. X-Ray patterns of pure CuO and  $\text{Ag}_2\text{O}/\text{CuO}$  were recorded in the  $2\theta$  range of  $10\text{--}80^\circ$  and depicted in Fig. 2(a and b). The diffraction lines for CuO were found at  $2\theta$  values of  $32.7^\circ$ ,  $35.4^\circ$ ,  $36.1^\circ$ , and  $39.3^\circ$  that agreed well with standard diffraction values for monoclinic CuO with planes (110), (002), ( $-111$ ), (200) (JCPDS File no. 01-080-0076) [ref]. The characteristic diffraction peaks of  $\text{Ag}_2\text{O}$  were observed at  $2\theta$  values of  $26.75^\circ$ ,  $33.9^\circ$ ,  $38.2^\circ$  and  $46.7^\circ$  that matched well with the JCPDS File no. 00-001-1041 of cubic  $\text{Ag}_2\text{O}$ . Sharp peaks were

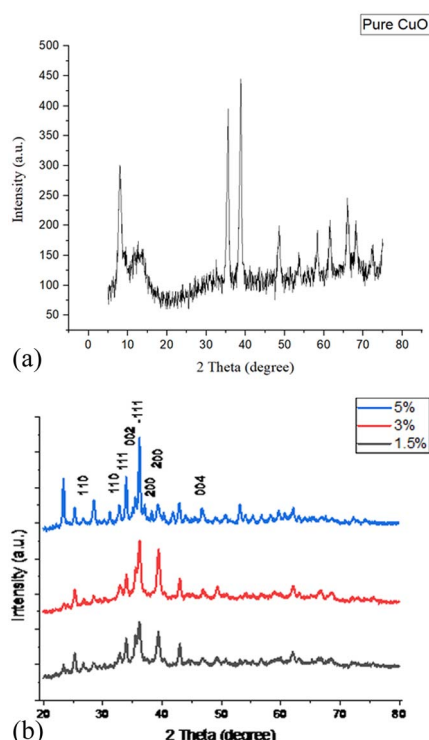


Fig. 2 (a) XRD patterns pure CuO nanoparticles. (b) XRD patterns of  $\text{Ag}_2\text{O}/\text{CuO}$  composite.

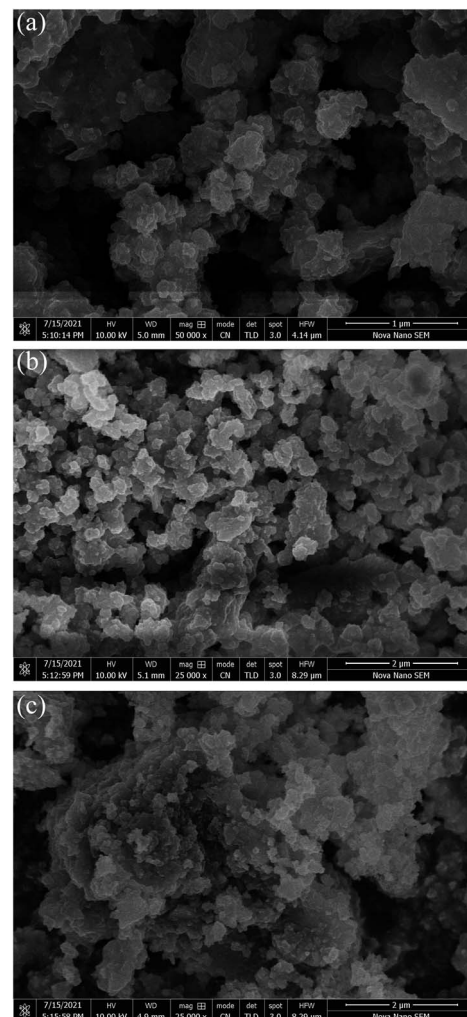


Fig. 3 SEM images of  $\text{Ag}_2\text{O}$  doped CuO composites (a: 1.5%  $\text{Ag}_2\text{O}/\text{CuO}$ , b: 3%  $\text{Ag}_2\text{O}/\text{CuO}$  and c: 5%  $\text{Ag}_2\text{O}/\text{CuO}$ ).

observed for  $\text{Ag}_2\text{O}/\text{CuO}$  composites that evidenced the absence of any impurity in the sample. The average particle size observed was in the range of  $20\text{--}35$  nm which was determined by Scherer calculations using X-pert Highscore software.<sup>23,24</sup> The Scanning Electron Micrograph of  $\text{Ag}_2\text{O}/\text{CuO}$  is presented in Fig. 3. The figure clearly showed agglomerated spherical particles. The presence of  $\text{Ag}_2\text{O}$  in  $\text{Ag}_2\text{O}/\text{CuO}$  turned the samples into more homogeneous ones. The EDX study confirmed the formation of  $\text{Ag}_2\text{O}/\text{CuO}$  composites as depicted in Fig. 4. The peaks represent the presence of Ag followed by Cu and O. Different elemental proportions of Ag were observed in the analysis which confirmed the different doping concentrations.<sup>23</sup>

The IR spectrum of  $\text{Ag}_2\text{O}/\text{CuO}$  composites is presented in Fig. 5. The vibrations around  $400\text{ cm}^{-1}$  to  $600\text{ cm}^{-1}$  are characteristic of Cu–O and Ag–O. The vibration observed at  $1600\text{ cm}^{-1}$  is due to the bending vibrations of absorbed water molecules. The vibrations observed at  $1370\text{ cm}^{-1}$  are attributed to the longitudinal phonon, which is similar to the character commonly possessed by nanoparticles.<sup>24–26</sup> The bands at  $1160$  and  $1100\text{ cm}^{-1}$  were assigned to C–O stretching vibrations.<sup>27</sup>



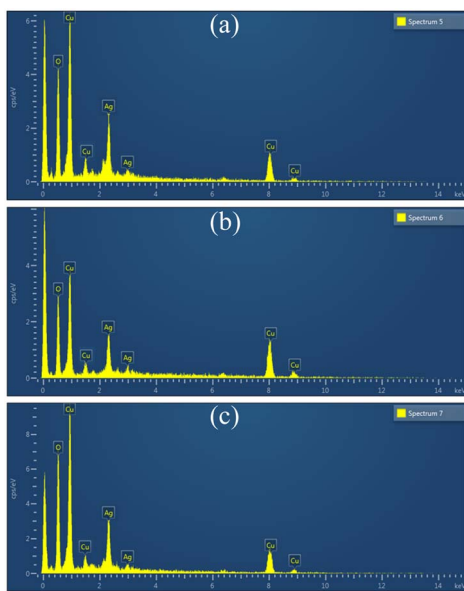


Fig. 4 EDX of  $\text{Ag}_2\text{O}$  doped  $\text{CuO}$  composites (a: 1.5%  $\text{Ag}_2\text{O}/\text{CuO}$ , b: 3%  $\text{Ag}_2\text{O}/\text{CuO}$  and c: 5%  $\text{Ag}_2\text{O}/\text{CuO}$ ).

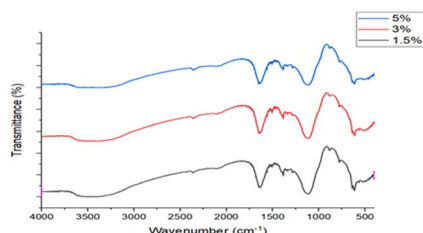


Fig. 5 FT-IR spectrum of  $\text{Ag}_2\text{O}$  doped  $\text{CuO}$  nanoparticles.

The thermal stability of  $\text{Ag}_2\text{O}/\text{CuO}$  composites was investigated by thermogravimetric analysis as depicted in Fig. 6. Small weight loss was observed up to a temperature of 100 °C that was attributed to the removal of moisture present on the surface of composites. The weight loss observed in the range of 600–900 °C was due to the loss of solvent molecules trapped in the crystal lattice. After 900 °C no more weight loss was observed.<sup>28</sup> All the compositions followed the same pattern.

### Photoluminescence (PL) analysis

Photoluminescence (PL) study of  $\text{CuO}$  and  $\text{Ag}_2\text{O}$  doped  $\text{CuO}$  composites are depicted in Fig. 7. The figure shows two dominant emission peaks for  $\text{CuO}$  centered at 416 nm and 475 nm that are attributed to the green emission produced from electronic transitions of ionized oxygen vacancies. However, in the case of  $\text{Ag}_2\text{O}$  doped  $\text{CuO}$  composites the peak at 416 nm is shifted to 405 nm. The figure clearly shows a decrease in the intensity after doping with silver. Furthermore, the intensity of peak was decreased with increase in the concentration of  $\text{Ag}_2\text{O}$ . These results are explained on the basis of fact that presence of Ag in the composite changes the size of the crystallites due to its amorphous nature. Therefore, for  $\text{Ag}_2\text{O}$  doped  $\text{CuO}$  composites,

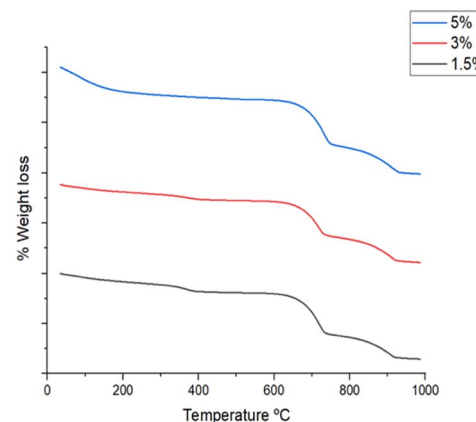


Fig. 6 TGA curve of  $\text{Ag}_2\text{O}$  doped  $\text{CuO}$  nanoparticles.

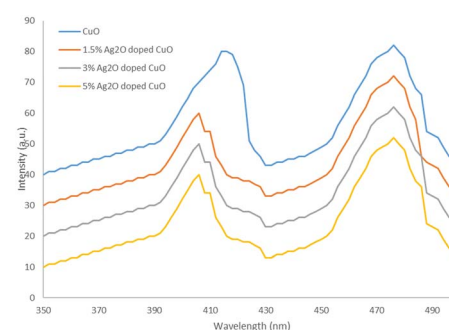


Fig. 7 Photo luminescence spectra of different compositions of  $\text{Ag}_2\text{O}$  doped  $\text{CuO}$  catalyst.

the rate of electron–hole recombination becomes lower as compared to  $\text{CuO}$  this rate is reduced with increase in concentration of Ag.<sup>29,30</sup> Thus 5%  $\text{Ag}_2\text{O}$  doped  $\text{CuO}$  was better photocatalyst.

### Photocatalytic degradation of imidacloprid by $\text{Ag}_2\text{O}/\text{CuO}$ composite

The photocatalytic degradation of imidacloprid was studied by optimizing various parameters such as time, catalyst dose, the concentration of pesticide, temperature, and pH in the presence of  $\text{Ag}_2\text{O}/\text{CuO}$  as a catalyst.

### Optimum composition of the catalyst

The presence of silver in  $\text{Ag}_2\text{O}/\text{CuO}$  affected the degradation efficiency of copper oxide. The silver ions play the role of the sink for the photo-excited electrons from the semiconductor. The separation efficiency of holes and photo-excited electron is also improved as the silver ions also play a role in the inhibition of charge recombination.<sup>31</sup> It was also found that photocatalytic activity of  $\text{Ag}_2\text{O}/\text{CuO}$  was increased by increasing the silver concentration from 1.5% to 5%. After optimum concentrations, the degradation efficiency was reduced due to oxygen defects. Tariq *et al.* 2019, calculated the degradation efficiency of Ag doped  $\text{ZnO}$  with Ag doping of 3% to 7% and a decrease in



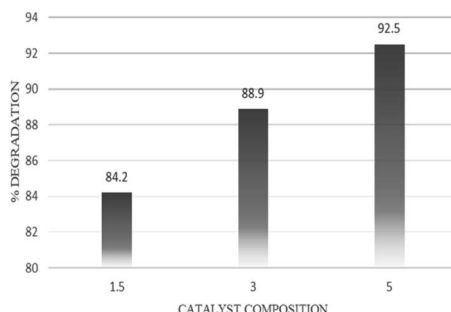


Fig. 8 Degradation of imidacloprid with different compositions of  $\text{Ag}_2\text{O}/\text{CuO}$  composite.

degradation efficiency was observed after optimum concentration. Fig. 8 depicted the degradation efficiency of different  $\text{Ag}_2\text{O}/\text{CuO}$  composites. The maximum degradation of imidacloprid was observed with 5%  $\text{Ag}_2\text{O}/\text{CuO}$  which was found to be 92.5%.<sup>32</sup> Therefore, this composition of catalyst was used throughout the study.

#### Effect of time

The appropriate time for the photocatalytic degradation of imidacloprid was determined by adding 0.02 g of 5%  $\text{Ag}_2\text{O}$  doped  $\text{CuO}$  composite to 25 mL of imidacloprid solution and stirring the samples for different time intervals ranging from 1–5 hours. Fig. 8 depicts the data for the imidacloprid degradation in the absence of a catalyst under UV light and dark. The corresponding data for the experiments conducted in the presence of a catalyst are also furnished in Fig. 9. The data showed that in the absence of catalyst, a 21.8% degradation of imidacloprid was observed in dark. Under UV irradiation, the extent of degradation was enhanced to 27.4%.

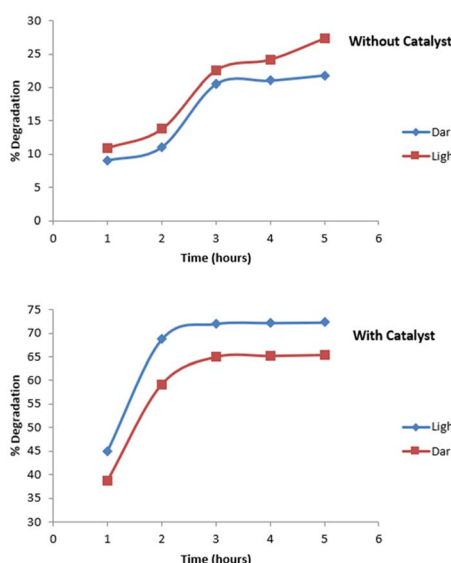


Fig. 9 Effect of time on the degradation of imidacloprid.

So, UV irradiation slightly promoted the degradation process. The presence of the catalyst significantly enhanced the degradation of imidacloprid even under dark conditions *i.e.*, 65% of imidacloprid degraded under dark which was increased to 72% under UV irradiation for 3 hours. After 3 hours, no major increase in the degradation of imidacloprid was observed. It is also worth noting that the degradation pattern observed in the presence of a catalyst was different from one observed in the absence of the catalyst. In the absence of the catalyst, the degradation first increased slowly up to 2 hours, and then it rapidly increased up to 3 hours. Afterwards, little or no degradation was observed. In the presence of the catalyst, a rapid increase in degradation was observed for up to 2 hours. After this, a non-significant increase in degradation was observed. The main advantage of this process is the relatively lower reaction time that leads to a reduction in the construction and operating costs.<sup>33</sup>

#### Effect of concentration of pesticide

The data for degradation of different concentrations of imidacloprid is provided in Fig. 10. It was found that the maximum degradation of 74.3% was observed for  $10 \text{ mg L}^{-1}$  of imidacloprid under UV light and 67% under dark. The percentage degradation of imidacloprid was decreased by increasing its concentration. It was attributed to the increased equilibrium adsorption on active catalyst sites.<sup>32,34</sup>

#### Effect of dose of catalyst

The data for degradation of imidacloprid solution ( $10 \text{ mg L}^{-1}$ ) by using different amounts of catalyst *i.e.*, 0.01, 0.02, 0.03, 0.04, and 0.05 g, is presented in Fig. 11. The maximum degradation (80.7%) of imidacloprid was observed with 0.01 g of catalyst in the presence of UV light and 77.4% under dark conditions.

By increasing the catalyst dose from optimal amount, the degradation efficiency was observed to be reduced due to the clustering of  $\text{Ag}_2\text{O}/\text{CuO}$  particles that consequently resulted in a decreased available sites on the catalyst surface. The increased catalyst concentration also reduced the light penetration due to the turbidity of the medium that also led to reduced degradation.<sup>35</sup>

#### Effect of pH

The data for degradation of  $10 \text{ mg L}^{-1}$  imidacloprid at different pH values is depicted in Fig. 12 which showed a maximum

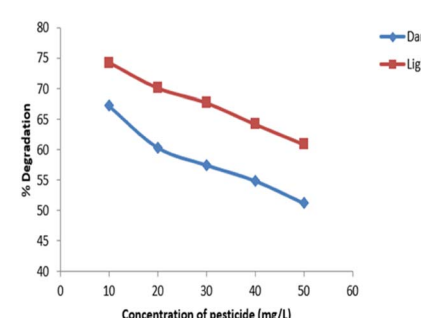


Fig. 10 Effect of concentration of imidacloprid on its degradation.



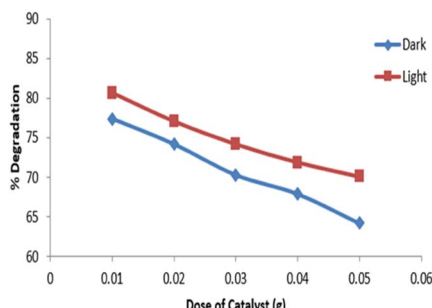


Fig. 11 Effect of catalyst dose on degradation of imidacloprid.

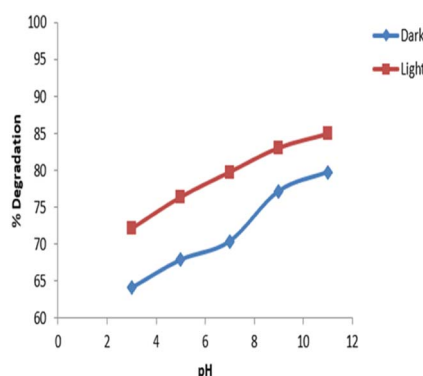
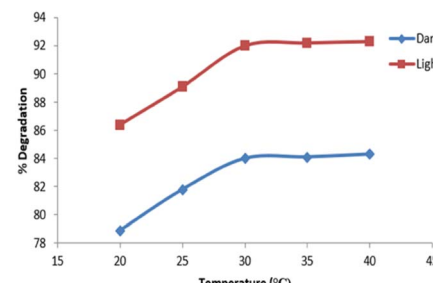
degradation of 85% in the presence of UV light and 79.8% under dark condition at a pH 11. The minimum degradation was observed at pH 3 which was 64.1% under dark and 72.15% in the presence of UV light.

The degradation of imidacloprid was increased at higher pH due to the increased  $\text{OH}^-$  concentration that increased the hydrolysis of imidacloprid. A  $-\text{C}=\text{N}-$  bond couples with electron-withdrawing  $-\text{NO}_2$  group of imidazolidine ring creating a small positive charge that reacts with  $\text{OH}$  ions in solution due to high pH thus increasing the hydrolysis and extent of degradation. The degradation of imidacloprid was also studied by Thuyet *et al.* at pH 7 and 10. A faster degradation was observed at pH 10 as compared to 7. At pH 10, the concentration of imidacloprid dropped by 48% as compared to 12% at pH 7 in paddy water.<sup>36</sup> Similarly, in the present study, degradation of 64.1% was observed under dark at pH 3 that was increased with an increase in pH approaching an optimum at pH 11.

### Effect of temperature

The degradation of  $10 \text{ mg L}^{-1}$  imidacloprid solution containing  $0.01 \text{ g}$  catalyst was studied at various temperatures *i.e.*,  $20^\circ\text{C}$ ,  $25^\circ\text{C}$ ,  $30^\circ\text{C}$ ,  $35^\circ\text{C}$ , and  $40^\circ\text{C}$  under optimum conditions. Each sample was stirred for 3 hours in the presence of UV light and under dark. The relevant data is depicted in Fig. 13.

The maximum degradation was observed for samples maintained at  $30^\circ\text{C}$  both in the presence of UV light and dark.

Fig. 12 Effect of pH on degradation of imidacloprid using  $\text{Ag}_2\text{O}$  doped  $\text{CuO}$  catalyst.Fig. 13 Effect of temperature on the degradation of imidacloprid by using  $\text{Ag}_2\text{O}$  doped  $\text{CuO}$  catalyst.

The degradation efficiency increased first with increasing temperature. After an optimum temperature, there was no increase in degradation efficiency with temperature. Patil *et al.* studied the degradation of imidacloprid at temperatures above  $30^\circ\text{C}$  and found the extent of degradation to be 12.85%, 12.69%, and 12.54% at operating temperatures of  $34^\circ\text{C}$ ,  $39^\circ\text{C}$ , and  $42^\circ\text{C}$  respectively.<sup>37</sup> Our studies also showed that the degradation efficiency increases till the optimum temperature is achieved. At  $30^\circ\text{C}$  the extent of degradation observed was 92%. Afterwards, no further increase in degradation was observed.

### Kinetic study of photocatalytic degradation of imidacloprid

The imidacloprid degradation was observed for 30–300 minutes by following first-order kinetics as depicted in Fig. 14. It is evident from the data that without a catalyst, the degradation rate of imidacloprid was  $0.036 \text{ h}^{-1}$  under dark conditions while it was  $0.045 \text{ h}^{-1}$  under UV light. Thus, the half-life of imidacloprid under these conditions was 19.25 hours under dark which was reduced to 15.4 hours under the influence of UV light. The presence of  $\text{Ag}_2\text{O}/\text{CuO}$  catalyst facilitated the degradation of imidacloprid both in the presence of UV light and dark. It is evident from the data that the rate of degradation in the presence of the catalyst under dark was  $0.068 \text{ h}^{-1}$  which yielded a half-life of 10.19 hours that was quite lower as compared to that noted under similar conditions in the absence

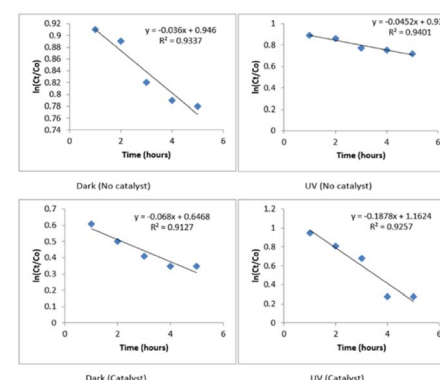


Fig. 14 Degradation kinetics of imidacloprid.



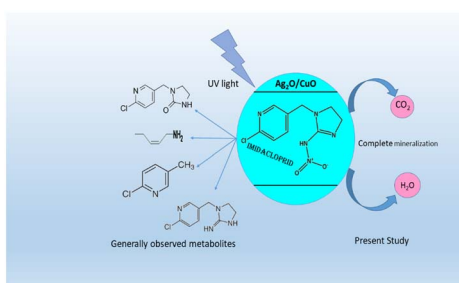


Fig. 15 Schematic diagram of photocatalytic degradation of imidacloprid by using silver oxide doped copper oxide catalyst.

of the catalyst. UV irradiation further enhanced the process of degradation and reduced the half-life to 3.7 hours as the rate of reaction was increased to  $0.187 \text{ h}^{-1}$ . Yari *et al.* (2019) degraded imidacloprid using  $\text{ZnO}$  and  $\text{TiO}_2$ , where the half-life was calculated to be 4.5 hours. In the case of  $\text{Ag}_2\text{O}/\text{CuO}$  composite (present study), the half-life observed was 3.70 hours which showed better degradation efficiency<sup>35</sup> of present catalyst.

GC-MS analysis was carried out to study the possible degradation products of imidacloprid and to get an insight into its degradation pathway. It is worth noting that no metabolites of imidacloprid were observed and the present catalyst was capable of bringing out the complete mineralization of imidacloprid. The schematic diagram for pesticide degradation in the presence of  $\text{Ag}_2\text{O}/\text{CuO}$  nanoparticles is elaborated in Fig. 15.<sup>38</sup>

The  $\text{CuO}$  nanoparticles exhibit a narrow bandgap of 1.2 eV which offers easy recombination of photo-generated electron-hole pairs. But, the doping of silver improves the band gap to 2.6 eV which restricts the electron-hole recombination rate and improves the charge separation.<sup>39,40</sup>

### Scavenger studies

The reactive species such as electrons, holes, superoxide radicals and hydroxyl radicals are responsible for determining the mechanism of the photodegradation. The role of these reactive species on the degradation of imidacloprid was studied by using different scavengers for an initial imidacloprid concentration of  $20 \text{ mg L}^{-1}$ . At this concentration, the photo-degradation efficiency was observed to be 92% in the presence of UV light. The data in Table 1 depicted that the degradation efficiency was decreased in the presence of electrons and superoxide radical scavengers *i.e.*  $\text{K}_2\text{Cr}_2\text{O}_7$ , 1,4 benzoquinone and isopropyl alcohol. While in the presence of formic acid ( $\text{h}^+$  scavenger), the degradation of imidacloprid was increased to 99%. In conclusion,  $\text{h}^+$  scavengers allowed the electrons to react with the pollutant resulting in lowering of the recombination rate of electron-hole charge carriers leading to better degradation efficiency.<sup>41,42</sup>

### Reusability of the catalyst

The catalyst was reused for three successive cycles to determine its stability and activity. The catalyst was primarily used for

Table 1 Effect of different scavengers on degradation of imidacloprid

Scavengers	Radicals	% Degradation
Without scavengers	—	92
Formic acid 20 mM	$\text{h}^+$	99
Isopropyl alcohol 1 M	$\text{HO}^\cdot$	70
$\text{K}_2\text{Cr}_2\text{O}_7$ 1 mM	$\text{e}^-$	35
1,4 Benzoquinone 1 mM	$\text{O}_2^\cdot-$	45

degradation at optimum conditions that provided maximum degradation of 92.3%. It was then filtered, washed thoroughly and dried at  $100^\circ\text{C}$ . After drying the catalyst was reused at optimum conditions and the degradation observed was 78%. The catalyst was reused again after activation by using the same procedure and the degradation observed for the third cycle was 63.41% as shown in Fig. 16. The stability of the catalyst was studied by leaching experiments. The catalyst was soaked in acidic conditions for 4 hours and no concentration of Cu and Ag was detected in the solution as checked by Atomic absorption spectrophotometer. The XRD spectra of catalyst after three cycles is shown in Fig. 17. The XRD patterns revealed the structural stability of the catalyst. The decrease in activity of the catalyst after three cycles is due to the agglomeration of particles which reduces the surface area.<sup>43</sup> Furthermore, the adsorption of imidacloprid molecules within the pores of catalyst is another factor which blocks some of the active sites and thus decreases the efficiency of the catalyst.

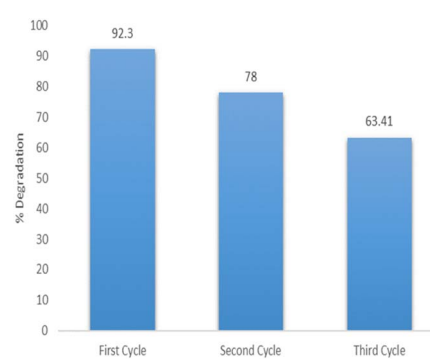


Fig. 16 Reusability study of  $\text{Ag}_2\text{O}$  doped  $\text{CuO}$  catalyst.

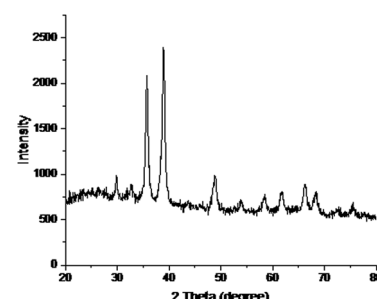


Fig. 17 XRD pattern of  $\text{Ag}_2\text{O}$  doped  $\text{CuO}$  catalyst after three reaction cycles.



## Conclusions

The present study focused on the preparation of a highly effective catalyst  $\text{Ag}_2\text{O}/\text{CuO}$  that was used for degradation of imidacloprid. The maximum degradation of imidacloprid was observed for  $10 \text{ mg L}^{-1}$  imidacloprid solution with  $0.01 \text{ g}$  catalyst at pH 11 in the presence of UV light. The optimum temperature for the degradation process was found to be  $30^\circ\text{C}$ . The efficiency of  $\text{Ag}_2\text{O}/\text{CuO}$  was found to be 92.3% and 84.3% in UV light and dark at optimum conditions. The prepared catalyst was effective in reducing the half-life of imidacloprid to 3.7 hours under UV light. The catalyst was able to be reused for up to 3 cycles with slight reduction in activity. The catalyst was able to maintain its structural integrity even after use in three consecutive cycles. The stability studies showed that the catalyst was also stable during the reaction course as evidenced by no detectable leaching of either Ag or Cu by Atomic absorption spectrophotometer. Thus,  $\text{Ag}_2\text{O}/\text{CuO}$  may be used as an efficient material for removing the pollutants like imidacloprid from contaminated aqueous environments.

## Author contributions

Saadia Rashid Tariq planned, supervised, edited and finalized the whole project. Zunaira Niaz performed experimental work and initial write up, formatting and editing. Ghayoor Abbas and Dildar Ahmed provided the instrumental facilities for material characterization and testing. Nazia Rafique reviewed the paper.

## Conflicts of interest

There are no conflicts to declare.

## Acknowledgements

The authors acknowledge the chemicals provided by the Department of Chemistry, Lahore College for Women University, Lahore to carry out this research work. We are also thankful to Mr Zajif from LUMS, Lahore for carrying out the XRD and SEM-EDX analyses.

## References

- 1 K. Atacan, N. Güy, M. Ozmen and M. Özcar, *Applied Surface Science Advances*, 2021, **6**, 100156.
- 2 R. Mukhopadhyay, B. Sarkar, E. Khan, D. S. Alessi, J. K. Biswas, K. M. Manjaiah, M. Eguchi, K. C. W. Wu, Y. Yamauchi and Y. S. Ok, *Crit. Rev. Environ. Sci. Technol.*, 2022, **52**, 2611–2660.
- 3 M. S. S. Adam, S. Sikander, M. T. Qamar, S. Iqbal, A. Khalil, A. M. Taha, O. S. Abdel-Rahman and E. B. Elkaeed, *Front. Chem.*, 2023, **11**, 1125835.
- 4 T. Kobkeatthawin, J. Trakulmututa, T. Amornsakchai, P. Kajitvichyanukul and S. M. Smith, *Catalysts*, 2022, **12**(2), 120.
- 5 S. Pang, Z. Lin, Y. Zhang, W. Zhang, N. Alansary, S. Mishra, P. Bhatt and S. Chen, *Toxics*, 2020, **8**(3), 1–31.
- 6 R. Garg, R. Gupta and A. Bansal, *Int. J. Environ. Sci. Technol.*, 2021, **18**, 1425–1442.
- 7 K. Babic, V. Tomašić, V. Gilja, J. Le Cunff, V. Gomzi, A. Pintar, G. Žerjav, S. Kurajica, M. Duplancic, I. E. Zelic, T. V. Pavicic and I. Grcic, *J. Environ. Chem. Eng.*, 2021, **9**, 105611.
- 8 A. Qayyum, I. A. Bhatti, A. Ashar, A. Jilani, J. Iqbal, M. Mohsin, T. Ishaq, S. Muhammad, S. Wageh and M. R. Dustgeer, *Polymers*, 2022, **14**(2), 295.
- 9 B. Ruomeng, O. Meihao, Z. Siru, G. Shichen, Z. Yixian, C. Junhong, M. Ruijie, L. Yuan, X. Gezhi, C. Xingyu, Z. Shiyi, Z. Aihui and F. Baishan, *Synth. Syst. Biotechnol.*, 2023, **8**, 302–313.
- 10 D. D. Nguyen, K. A. Huynh, X. H. Nguyen and T. P. Nguyen, *Res. Chem. Intermed.*, 2020, **46**, 4823–4840.
- 11 F. S. Bruckmann, C. Schnorr, L. R. Oviedo, S. Knani, L. F. O. Silva, W. L. Silva, G. L. Dotto and C. R. Bohn Rhoden, *Molecules*, 2022, **27**, 6261.
- 12 A. Massoud, A. Derbalah, I. El-Mehasseb, M. S. Allah, M. S. Ahmed, A. Albrakati and E. K. Elmahallawy, *Int. J. Environ. Res. Public Health*, 2021, **18**(17), 9278.
- 13 E. F. A. Zeid, I. A. Ibrahim, W. A. A. Mohamed and A. M. Ali, *Mater. Res. Express*, 2020, **7**, 026201.
- 14 A. Iqbal, A. U. Haq, G. A. Cerrón-Calle, S. A. R. Naqvi, P. Westerhoff and S. Garcia-Segura, *Catalysts*, 2021, **11**(7), 806.
- 15 K. Bano, S. Kaushal and P. P. Singh, *Polyhedron*, 2021, **209**, 115465.
- 16 S. Merci, A. Saljooqi, T. Shamspur and A. Mostafavi, *Environ. Sci. Pollut. Res.*, 2021, **28**, 35764–35776.
- 17 G. Murugadoss, N. Kandhasamy, M. Rajesh Kumar, A. K. Alanazi, F. Khan, B. Salhi and H. M. Yadav, *Inorg. Chem. Commun.*, 2022, **137**, 109186.
- 18 V. Srivastava, E. N. Zare, P. Makvandi, X. qi Zheng, S. Iftekhar, A. Wu, V. V. T. Padil, B. Mokhtari, R. S. Varma, F. R. Tay and M. Sillanpaa, *Chemosphere*, 2020, **258**, 127324.
- 19 M. Shkir, B. Palanivel, A. Khan, M. Kumar, J. H. Chang, A. Mani and S. AlFaify, *Chemosphere*, 2022, **291**(2), 132687.
- 20 M. Lal, P. Sharma, L. Singh and C. Ram, *Results Eng.*, 2023, **17**, 100890.
- 21 J. Lang, J. Wang, Q. Zhang, X. Li, Q. Han, M. Wei, Y. Sui, D. Wang and J. Yang, *Ceram. Int.*, 2016, **42**, 14175–14181.
- 22 L. S. J. Al-hayder and M. H. J. Al-juboory, *J. Chem. Pharm. Res.*, 2015, **7**(12), 1138–1144.
- 23 K. Jemal, B. V. Sandeep and S. Pola, *J. Nanomater.*, 2017, **2017**, 4213275.
- 24 L. S. Wang, J. C. Deng, F. Yang and T. Chen, *Mater. Chem. Phys.*, 2008, **108**, 165–169.
- 25 R. S. Ganesh, M. Navaneethan, V. L. Patil, S. Ponnusamy, C. Muthamizhchelvan, S. Kawasaki, P. S. Patil and Y. Hayakawa, *Sens. Actuators, B*, 2018, **255**(1), 672–683.
- 26 M. Maruthupandy, Y. Zuo, J. S. Chen, J. M. Song, H. L. Niu, C. J. Mao, S. Y. Zhang and Y. H. Shen, *Appl. Surf. Sci.*, 2017, **397**, 167–174.
- 27 M. Moradi, M. Haghghi and S. Allahyari, *Process Saf. Environ. Prot.*, 2017, **107**, 414–427.
- 28 P. G. Bhavyasree and T. S. Xavier, *Heliyon*, 2020, **6**, e03323.



29 A. A. Menazea and A. M. Mostafa, *J. Environ. Chem. Eng.*, 2020, **8**, 104104.

30 C. Tamuly, I. Saikia, M. Hazarika and M. R. Das, *RSC Adv.*, 2014, **4**, 53229–53236.

31 G. Murugadoss, D. D. Kumar, M. R. Kumar, N. Venkatesh and P. Sakthivel, *Sci. Rep.*, 2021, **11**, 1–13.

32 M. Kanwal, S. R. Tariq and G. A. Chotana, *Environ. Sci. Pollut. Res.*, 2018, **25**, 27307–27320.

33 K. Yari, A. Seidmohammadi, M. Khazaei, A. Bhatnagar and M. Leili, *J. Environ. Health Sci. Eng.*, 2019, **17**, 337–351.

34 F. Soltani-nezhad, A. Saljooqi, T. Shamspur and A. Mostafavi, *Polyhedron*, 2019, **165**, 188–196.

35 K. Yari, A. Seidmohammadi, M. Khazaei, A. Bhatnagar and M. Leili, *J. Environ. Health Sci. Eng.*, 2019, **17**, 337–351.

36 D. Q. Thuyet, H. Watanabe and J. Ok, *J. Pestic. Sci.*, 2013, **38**, 223–227.

37 P. N. Patil, S. D. Bote and P. R. Gogate, *Ultrason. Sonochem.*, 2014, **21**, 1770–1777.

38 D. Li, J. Li, B. Yeerhazi and Y. Cheng, *J. Chem. Technol. Biotechnol.*, 2023, **98**, 1014–1024.

39 R. Wang, G. Shan, T. Wang, D. Yin and Y. Chen, *J. Alloys Compd.*, 2021, **864**, 158591.

40 S. Vikal, A. Kumar, A. Kumar, N. Singh, H. Singh, B. P. Singh and Y. K. Gautam, *Nano Express*, 2023, **4**(2), 025004.

41 L. Andronic, A. Vladescu and A. Enesca, *Nanomaterials*, 2021, **11**(12), 3197.

42 W. Li, F. Wang, Y. Shi and L. Yu, *Chin. Chem. Lett.*, 2023, **34**(1), 107505.

43 A. K. Sibhatu, G. K. Weldegebrieal, S. Sagadevan, N. N. Tran and V. Hessel, *Chemosphere*, 2022, **300**, 134623.

